Radiation from a Center-Fed Cylindrical Antenna Surrounded by a Plasma Sheath

JAMES J. CAMPBELL

Abstract—The radiation field of a plasma-clad cylindrical antenna fed across an infinitesimal gap has been derived. The limitations on the validity of the far-field pattern have been stated. In the vicinity of the antenna, but in the region far from the gap, an expression is derived for the surface wave contribution which is the major source of field strength in this region. Analysis of the contour integration and discussion of the location of the various types of poles of the integrand on their appropriate Riemann sheets are presented.

Numerical computations of far-field patterns and surface wave fields are presented graphically.

Introduction

THE FORMATION of an ionized gaseous medium about space vehicles which are passing through the atmosphere at high velocities has been known for some time and has motivated numerous authors to investigate the effects of such plasmas on antenna radiation patterns.

The present paper discusses the problem of an infinite cylindrical antenna which is fed across an infinitesimal gap and which is surrounded by a thin plasma sheath. This type of excitation has been used frequently with high velocity vehicles where the entire vehicles approximated a large cylindrical antenna fed at the center across a small gap.

In a number of previous endeavors two approximations have been made which are also used in the present study. First it is assumed that the plasma is cold and there is no applied steady magnetic field. Under this assumption the plasma can be modeled as a dielectric medium with a scalar dielectric constant $\epsilon_p = \epsilon_0(1-\omega_p^2/\omega^2)$. Secondly, it is assumed that the sheath which surrounds the vehicle is homogeneous. Thus, the problem under consideration reduces to that of an infinite cylindrical antenna fed across an infinitesimal gap which is coated with homogeneous dielectric material.

The structure is closely related to that of a slot excited infinite cylindrical dielectric coated antenna which has been studied by numerous authors.[1-5] The major difference is the form of the assumed source excitation. The problem is formulated in terms of Hertz potentials and the far-field pattern is evaluated by the method of steepest descent. In addition to the space wave a study has been made of the surface waves which are excited on the cylinder. Numerical computations of the surface wave fields in the vicinity of the plasma-air interface have been performed.

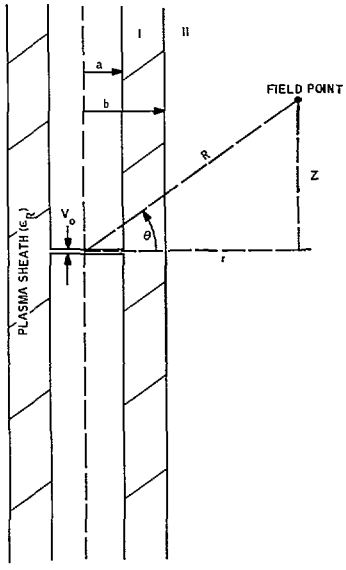

Fig. 1. Cylindrical geometry.

Far-Field Calculations

The geometry of the problem is depicted in Fig. 1. Problems of this sort are best handled by Hertz vectors. Due to the cylindrical geometry and the symmetry of the structure, only z components of π and π^* are required to match boundary conditions. Further, the source specifies the polarization of the exciting field to be TM (no H_z). Assuming that the response is also TM, then only the z component of the electric Hertz vector π_z is necessary to define the field and enable all boundary conditions to be satisfied.

The equation for π_z in regions I and II are:

$$\nabla^2\pi_z + K_0^2\epsilon_R\pi_z = 0 \quad \text{(Region I)} \tag{1}$$

$$\nabla^2\pi_z + K_0^2\pi_z = 0 \quad \text{(Region II)} \tag{2}$$

where ϵ_R is the relative permittivity of the plasma and K_0 is the propagation constant in free space. An $e^{-i\omega t}$ time dependence is used. A voltage drop V_0 is maintained across the infinitesimal gap so that the field in the gap is given by $E(z) = V_0\delta(z)$, $\delta(z)$ being the Dirac delta-function.

Manuscript received October 14, 1965.
The author is with ECM Systems Department, Philco Corp., Newport Beach, Calif.

[1] C. M. Knop, "The radiation fields from a circumferential slot on a metal cylinder coated with a lossy dielectric," *IRE Trans. on Antennas and Propagation*, vol. AP-9, pp. 535–545, November 1961.

[2] W. V. T. Rusch, "Radiation from an axially slotted cylinder with a radially inhomogeneous plasma coating," U.S.C.E.C. Rept. 82-210, March 1963.

[3] J. R. Wait, *Electromagnetic Radiation From Cylindrical Structures*. New York: Pergamon, 1959, pp. 125–138.

[4] G. Hasserjian, "Fields of a curved plasma layer excited by a slot," *IEEE Trans. on Antennas and Propagation*, vol. AP-13, pp. 389–395, May 1965.

[5] T. M. Smith and K. E. Golden, "Radiation patterns from a slotted cylinder surrounded by a plasma sheath," *IEEE Trans. on Antennas and Propagation*, vol. AP-13, pp. 775–780, September 1965.

Application of the usual method of separation of variables while noting the azimuthal symmetry of the problem yields solutions of the type

$$J_0(r\sqrt{K_0^2\epsilon_R - h^2})e^{\pm ihz}, \quad N_0(r\sqrt{K_0^2\epsilon_R - h^2})e^{\pm ihz},$$

$$J_0(r\sqrt{K_0^2 - h^2})e^{\pm ihz}, \text{ and } N_0(r\sqrt{K_0^2 - h^2})e^{\pm ihz}$$

The electric field and magnetic field are derived from the Hertz vector.

$$\vec{E} = \nabla \times \nabla \times \vec{\pi} \tag{5}$$

$$\vec{H} = \nabla \times \left(\epsilon_0\epsilon_R \frac{\partial \vec{\pi}}{\partial t}\right). \tag{6}$$

The indicated manipulations yield the following expressions.

$$\boldsymbol{E}^{\mathrm{I}} = \boldsymbol{u}_r\left[\int_{-\infty}^{\infty} c(h)\left\{ih\sqrt{K_0^2\epsilon_R - h^2}J_0'(r\sqrt{K_0^2\epsilon_R - h^2})\right\}e^{ihz}\,dh + \int_{-\infty}^{\infty} g(h)\left\{ih\sqrt{K_0^2\epsilon_R - h^2}N_0'(r\sqrt{K_0^2\epsilon_R - h^2})\right\}e^{ihz}\,dh\right]$$

$$+ \boldsymbol{u}_z\left[\int_{-\infty}^{\infty} c(h)\left\{(K_0^2\epsilon_R - h^2)J_0(r\sqrt{K_0^2\epsilon_R - h^2})\right\}e^{ihz}\,dh + \int_{-\infty}^{\infty} g(h)\left\{(K_0^2\epsilon_R - h^2)N_0(r\sqrt{K_0^2\epsilon_R - h^2})\right\}e^{ihz}\,dh\right] \tag{7}$$

$$\boldsymbol{E}^{\mathrm{II}} = \boldsymbol{u}_r\left[\int_{-\infty}^{\infty} f(h)\left\{ih\sqrt{K_0^2 - h^2}H_0'^{(1)}(r\sqrt{K_0^2 - h^2})\right\}e^{ihz}\,dh\right]$$

$$+ \boldsymbol{u}_z\left[\int_{-\infty}^{\infty} f(h)\left\{(K_0^2 - h^2)H_0^{(1)}(r\sqrt{K_0^2 - h^2})\right\}e^{ihz}\,dh\right] \tag{8}$$

$$\boldsymbol{H}^{\mathrm{I}} = \boldsymbol{u}_\phi(i\omega\epsilon_0\epsilon_R)\left[\int_{-\infty}^{\infty} c(h)\sqrt{K_0^2\epsilon_R - h^2}J_0'(r\sqrt{K_0^2\epsilon_R - h^2})e^{ihz}\,dh + \int_{-\infty}^{\infty} g(h)\sqrt{K_0^2\epsilon_R - h^2}N_0'(r\sqrt{K_0^2\epsilon_R - h^2})e^{ihz}\,dh\right] \tag{9}$$

$$\boldsymbol{H}^{\mathrm{II}} = \boldsymbol{u}_\phi(i\omega\epsilon_0)\int_{-\infty}^{\infty} f(h)\sqrt{K_0^2 - h^2}H_0'^{(1)}(r\sqrt{K_0^2 - h^2})e^{ihz}\,dh. \tag{10}$$

where h is not restricted. π_z in regions I and II, therefore, can be represented as a superposition of the above solutions to Maxwell's equations with undetermined coefficients $c(h)$, $g(h)$, and $f(h)$ as follows.

$$\pi_z^{\mathrm{I}}(r, z) = \int_{-\infty}^{\infty} c(h)J_0(r\sqrt{K_0^2\epsilon_R - h^2})e^{ihz}\,dh,$$

$$+ \int_{-\infty}^{\infty} g(h)N_0(r\sqrt{K_0^2\epsilon_R - h^2})e^{ihz}\,dh \tag{3}$$

$$\pi_z^{\mathrm{II}}(r, z) = \int_{-\infty}^{\infty} f(h)H_0^{(1)}(r\sqrt{K_0^2 - h^2})e^{ihz}\,dh. \tag{4}$$

$H_0^{(1)}(r\sqrt{K_0^2 - h^2})$ is used to represent an outgoing wave.

$\boldsymbol{u}_z$, $\boldsymbol{u}_r$, and $\boldsymbol{u}_\phi$ are unit vectors in the z, r, and ϕ directions. $c(h)$, $g(h)$, and $f(h)$ can be obtained by an application of the boundary conditions on the $\boldsymbol{E}$ and $\boldsymbol{H}$ fields. These are the following:

1) continuity of tangential component of $\boldsymbol{H}$ at $r = b(H_\phi)$
2) continuity of the tangential component of $\boldsymbol{E}$ at $r = b(E_z)$
3) E_z vanishing at $r = a$ except in the region of the gap where it must satisfy the source condition

$$E(z, a) = V_0\delta(z) = \frac{V_0}{2\pi}\int_{-\infty}^{\infty} e^{ihz}\,dh. \tag{11}$$

Application of these conditions yields the following set of equations.

$$\epsilon_R\sqrt{K_0^2\epsilon_R - h^2}J_0'(b\sqrt{K_0^2\epsilon_R - h^2})c(h) + \epsilon_R\sqrt{K_0^2\epsilon_R - h^2}N_0'(b\sqrt{K_0^2\epsilon_R - h^2})g(h)$$

$$- \sqrt{K_0^2 - h^2}H_0'^{(1)}(b\sqrt{K_0^2 - h^2})f(h) = 0 \tag{12}$$

$$(K_0^2\epsilon_R - h^2)J_0(b\sqrt{K_0^2\epsilon_R - h^2})c(h) + (K_0^2\epsilon_R - h^2)N_0(b\sqrt{K_0^2\epsilon_R - h^2})g(h) - (K_0^2 - h^2)H_0^{(1)}(b\sqrt{K_0^2 - h^2})f(h) = 0 \tag{13}$$

$$(K_0^2\epsilon_R - h^2)J_0(a\sqrt{K_0^2\epsilon_R - h^2})c(h) + (K_0^2\epsilon_R - h^2)N_0(a\sqrt{K_0^2\epsilon_R - h^2})g(h) = \frac{V_0}{2\pi}. \tag{14}$$

Solving these equations for $f(h)$ and recognizing the numerator as the Wronskian of N_0 and J_0, the following expression is obtained.

$$f(h) = \frac{V_0\epsilon_R/\pi^2 b\sqrt{K_0^2\epsilon_R - h^2}}{D(h)} \tag{15}$$

$$\begin{aligned} D(h) = {} & \sqrt{K_0^2 - h^2}H_0'^{(1)}(b\sqrt{K_0^2 - h^2})\left[K_0^2\epsilon_R - h^2\right]^{1/2} \\ & \cdot\left[J_0(b\sqrt{K_0^2\epsilon_R - h^2})N_0(a\sqrt{K_0^2\epsilon_R - h^2}) - J_0(a\sqrt{K_0^2\epsilon_R - h^2})N_0(b\sqrt{K_0^2\epsilon_R - h^2})\right] \\ & + \epsilon_R(K_0^2 - h^2)H_0^{(1)}(b\sqrt{K_0^2 - h^2}) \\ & \cdot\left[J_0(a\sqrt{K_0^2\epsilon_R - h^2})N_0'(b\sqrt{K_0^2\epsilon_R - h^2}) - N_0(a\sqrt{K_0^2\epsilon_R - h^2})J_0'(b\sqrt{K_0^2\epsilon_R - h^2})\right] \end{aligned} \tag{16}$$

$$H^{II} = u_\phi(i\omega\epsilon_0)\int_{-\infty}^{\infty} f(h)\sqrt{K_0^2 - h^2}H_0'^{(1)}(r\sqrt{K_0^2 - h^2})e^{ihz}\,dh \text{ from equation (10).}$$

Consider first the far-field ($r\sqrt{K_0^2-h^2}\gg 1$). For large values of $r\sqrt{K_0^2-h^2}$ the derivative of the Hankel function can be replaced by its asymptotic form

$$H_0'^{(1)}(\rho) \cong \sqrt{\frac{2}{\pi\rho}}\,e^{i[\rho+\pi/4]}. \tag{17}$$

Examination of the integral shows the existence of branch points at $h=\pm K_0$. There are no branch points associated with the $\sqrt{K_0^2\epsilon_R-h^2}$ terms in the integrand since the integrand is an even function of $\sqrt{K_0^2\epsilon_R-h^2}$.

The steepest descent[6,7] method is usually employed in the evaluation of integrals of this type. To simplify the integral further a transformation from the h plane to the ϕ plane is customarily employed. The transformation is as follows: $h=K_0\sin\phi$, $\phi=\xi+i\eta$. From Fig. 1, $r=R\cos\theta$ and $z=R\sin\theta$. Thus

$$H^{II} = u_\phi e^{i(\pi/4)}\sqrt{\frac{2}{\pi R\cos\theta}}\,(i\omega\epsilon_0)$$

$$\cdot\int_c f(K_0\sin\phi)\left[K_0\cos\phi\right]^{3/2}e^{iK_0R\cos(\theta-\phi)}\,d\phi \tag{18}$$

where the contour c is the original path of integration in the ϕ plane. There are branch points at $\phi=\pm\pi/2$ due to the $(\cos\phi)^{3/2}$ term in the integrand. The associated branch cut may be taken as shown in Fig. 2 and will not interfere with the steepest descent path. Similar branch cuts are taken at $\phi=\pm(2N+1)\pi/2$ where $N=1, 2, 3, \cdots$, and do not interfere with the steepest descent path.

The saddle point is at $\phi=\theta$. Simple manipulations show the steepest descent path to be defined as follows:

$$\cos(\theta-\xi)\cosh\eta = 1. \tag{19}$$

This is shown as c' in Fig. 2.

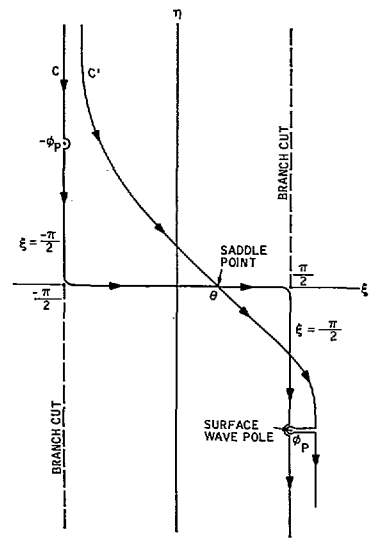

Fig. 2. Integration paths, ϕ plane.

The steepest descent integral has the form

$$\int_{c'} P(\phi)e^{iK_0R\cos(\theta-\phi)}\,d\phi = \int_{c'} e^{RQ(\phi)}\,d\phi.$$

$$Q(\phi) = \frac{\ln P(\phi)}{R} + iK_0\cos(\theta-\phi)\;Q(\phi)$$

where R is large. Along the steepest descent path $Q(\phi)=Q(\theta)-\omega^2$. Also

$$Q(\phi) = Q(\theta) + Q''(\theta)\frac{(\phi-\theta)^2}{2} + \cdots,$$

near the saddle point where the major contribution to the integral occurs. Thus

$$-\omega^2 \cong \frac{Q''(\theta)}{2}(\phi-\theta)^2 = -\frac{iK_0}{2}(\phi-\theta)^2.$$

[6] P. M. Morse and H. Feshbach, *Methods of Theoretical Physics*. New York: McGraw-Hill, 1953, pp. 437–443.

[7] R. E. Collin, *Field Theory of Guided Waves*. New York: McGraw-Hill, 1960, pp. 495–506.

From this it can be shown that

$$\int_{c'} P(\phi)e^{iK_0R\cos(\theta-\phi)}\,d\phi \cong e^{RQ(\theta)}e^{-i(\pi/4)}\sqrt{\frac{2}{K_0}}\int_{-\infty}^{\infty}e^{-R\omega^2}\,d\omega = e^{RQ(\theta)}e^{-i(\pi/4)}\sqrt{\frac{2\pi}{K_0R}}.$$

Thus

$$H_\phi(R,\theta) = \frac{2i\omega\epsilon_0K_0\cos\theta}{R}f(K_0\sin\theta)e^{iK_0R} \qquad (20)$$

or

$$H_\phi(R,\theta) = \frac{-2i\omega\epsilon_0\epsilon_RV_0e^{iK_0R}}{\pi^2K_0^2bRA(\theta)}. \qquad (21)$$

problems of this sort and the regions in the ϕ plane in which they may exist is given by Tamir and Oliner.[8] Their effect can be ignored in the far field when an evaluation by the steepest descent method is used.

In the vicinity of the antenna but far from the gap the major contribution to the field comes from the surface wave. The steepest descent integration is no longer valid. The integrand is proportional to $H_1^{(1)}(r\sqrt{K_0^2-h^2})$ and the steepest descent integration depends upon approximating the Hankel function by an exponential

$$H_1^{(1)}(r\sqrt{K_0^2-h^2}) \cong \sqrt{\frac{2}{\pi r\sqrt{K_0^2-h^2}}}\cdot e^{i(r\sqrt{K_0^2-h^2}-3\pi/4)}.$$

$$A(\theta) = H_1^{(1)}(K_0b\cos\theta)[\epsilon_R-\sin^2\theta]\cdot[J_0(K_0b\sqrt{\epsilon_R-\sin^2\theta})N_0(K_0a\sqrt{\epsilon_R-\sin^2\theta}) - J_0(K_0a\sqrt{\epsilon_R-\sin^2\theta})N_0(K_0b\sqrt{\epsilon_R-\sin^2\theta}) + \epsilon_R\cos\theta H_0^{(1)}(K_0b\cos\theta)\sqrt{\epsilon_R-\sin^2\theta}\cdot[J_0(K_0a\sqrt{\epsilon_R-\sin^2\theta})N_1(K_0b\sqrt{\epsilon_R-\sin^2\theta}) - N_0(K_0a\sqrt{\epsilon_R-\sin^2\theta})J_1(K_0b\sqrt{\epsilon_R-\sin^2\theta})]. \qquad (22)$$

Surface Waves

The surface wave contribution to the far field decays exponentially in the radial direction but propagates in the z direction. It contributes directly in the steepest descent method only if the pole is crossed in deforming the path of integration. Otherwise its contribution is included in the steepest descent integral (see Fig. 2). ϕ_p represents the surface wave pole that may be crossed in deforming the contour. This corresponds to a location in the ϕ plane along the line $\phi=\pi/2-i|\eta|$ below the point where the steepest descent path crosses this line. Along the steepest descent path $\cos(\xi-\theta)\cosh\eta=1$. It crosses $\phi=\pi/2-i|\eta|$ when $\cos(\pi/2-\theta)\cosh|\eta_0|=1$ [i.e., $|\eta_0|=\cosh^{-1}(\csc\theta)$]. The pole contributes directly if $|\eta_p|>|\eta_0|$.

The contribution of the surface wave pole in the far field is negligible, however, even if it is crossed in deforming the contour to the steepest descent path. This is due to the exponential decay of its residue in the radial direction. The same is true of other poles of the integrand that may be crossed in deforming the contour whether they be complex spectral or complex nonspectral poles. An excellent discussion of complex poles for

This approximation is valid only for large arguments. In order to be valid, $\sqrt{K_0^2-h^2}\gg1$, which is not true in the vicinity of the antenna. The integral could be done by taking the original path of integration in the h plane and closing the contour in the upper half plane being sure to loop around the branch cut so as to remain on the first Riemann sheet. The contour is shown in Fig. 3. In order to satisfy the radiation condition it is necessary that $IM(\sqrt{K_0^2-h^2})>0$. This condition defines the branch cut for the branch points $\pm K_0$ in the h plane. Allowing K_0 to have a small imaginary part to correspond to physical reality, the branch cut is as shown in Fig. 3. Complex poles on the upper Riemann sheet ($\mathrm{IM}(\sqrt{K_0^2-h^2})>0$) are of the proper or spectral type while those on the lower Riemann sheet ($\mathrm{IM}(\sqrt{K_0^2-h^2})<0$) are of the improper or nonspectral type. The integral goes to zero on the semicircle at ∞ due to the e^{ihz} factor in the integrand. Due to the e^{ihz} factor in the

[8] T. Tamir and A. A. Oliner, "The influence of complex waves on the radiation field of a slot-excited plasma layer," *IRE Trans. on Antennas and Propagation*, vol. AP-10, pp. 55–65, January 1962.

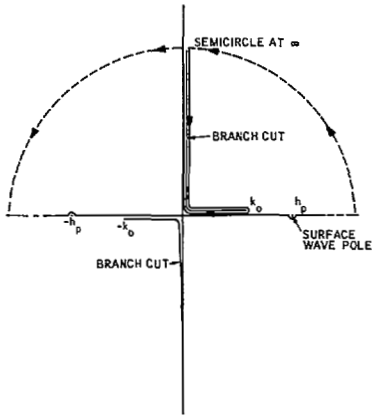

Fig. 3. Integration path, h plane.

integrand it becomes exponentially small along the branch cut also for large values of z. The branch cut integral will go as $1/z$ due to the e^{ihz} factor and will thus be small at large values of z compared to the surface wave contribution.

The integral along the real axis can be found by summing the residues of the poles in the upper half plane on sheet 1. Except for the surface wave pole the rest of the poles must be complex spectral whose contributions decay exponentially for large z. Thus the only contribution at large z and close to the surface will be the surface wave mode. Due to the axial symmetry only the TM mode exists. The contribution to the field of this mode is as follows:

Numerical Calculations and Discussion

Numerical data is presented graphically in the form of far-field patterns as a function of aspect angle and surface wave contributions as a function of distance from the plasma-air interface. The surface wave calculations were based on computations made by Rusch[9] of the location of poles representing various types of propagation modes on cylindrical plasma-clad surfaces. Forward waves only were considered. Another excellent source of numerical data on dispersion relationships for backward as well as forward waves is a paper by Tamir and Palocz.[10] The magnitude of the surface wave field can be written as a function of the following variables: $B=K_0b$, $P=a/b$, $\gamma=\omega/\omega_P$, $\delta=h_P/K_0$, r, and ω. The dependence on ω is linear and the r dependence enters only through $H_1^{(1)}(r\sqrt{K_0^2-h_P^2})$. The other terms in the expression are functions of B, P, γ, and δ only. Thus $\epsilon_R=1-1/\gamma^2$, $b\sqrt{K_0^2-h_P^2}=B\sqrt{1-\delta^2}$, etc. The quantity plotted then is

$$h_\phi(r)=\frac{|H_\phi(r,z)|}{2\omega\epsilon_0V_0/\pi}$$

as a function of r/b. Plots are made for various values of γ for fixed B and P. δ of course is fixed by the values of γ, B, and P. It can be seen that the most rapid decrease in field strength for a fixed ω occurs as ω_P decreases.

[9] W. V. T. Rusch, "Propagation constants of surface waves on a plasma-clad cylinder," *IRE Trans. on Antennas and Propagation (Communications)*, vol. AP-10, pp. 213–214, March 1962.

[10] T. Tamir and S. Palocz, "Surface waves on plasma-clad metal rods," *IEEE Trans. on Microwave Theory and Techniques*, vol. MTT-12, pp. 189–196, March 1964.

$$H\phi(r,z) = -2\omega\epsilon_0\epsilon_R V_0 H_1^{(1)}(r\sqrt{K_0^2-h_P^2})e^{ih_Pz}/\pi b\sqrt{K_0^2\epsilon_R-h_P^2}K(h_P) \tag{23}$$

$$\begin{aligned}K(h_P) = {} & \alpha'(h_P)[K_0^2\epsilon_R-h_P^2]^{1/2}H_1^{(1)}(b\sqrt{K_0^2-h_P^2})-h_P\alpha(h_P)[K_0^2\epsilon_R-h_P^2]^{-1/2}H_1^{(1)}(b\sqrt{K_0^2-h_P^2})\\ & -h_Pb\alpha(h_P)[K_0^2\epsilon_R-h_P^2]^{1/2}[K_0^2-h_P^2]^{-1/2}H_1'^{(1)}(b\sqrt{K_0^2-h_P^2})-\epsilon_R\beta'(h_P)[K_0^2-h_P^2]^{1/2}H_0^{(1)}(b\sqrt{K_0^2-h_P^2})\\ & +\epsilon_Rh_P\beta(h_P)[K_0^2-h_P^2]^{-1/2}H_0^{(1)}(b\sqrt{K_0^2-h_P^2})+\epsilon_Rh_Pb\beta(h_P)H_0'^{(1)}(b\sqrt{K_0^2-h_P^2})\end{aligned} \tag{24}$$

$$\alpha(h_P) = J_0(b\sqrt{K_0^2\epsilon_R-h_P^2})N_0(a\sqrt{K_0^2\epsilon_R-h_P^2})-J_0(a\sqrt{K_0^2\epsilon_R-h_P^2})N_0(b\sqrt{K_0^2\epsilon_R-h_P^2}) \tag{25}$$

$$\beta(h_P) = J_0(a\sqrt{K_0^2\epsilon_R-h_P^2})N_0'(b\sqrt{K_0^2\epsilon_R-h_P^2})-N_0(a\sqrt{K_0^2\epsilon_R-h_P^2})J_0'(b\sqrt{K_0^2\epsilon_R-h_P^2}) \tag{26}$$

$$\begin{aligned}\alpha'(h_P) = {} & -h_P(K_0^2\epsilon_R-h_P^2)^{-1/2}[aJ_0(b\sqrt{K_0^2\epsilon_R-h_P^2})N_0'(a\sqrt{K_0^2\epsilon_R-h_P^2})+bN_0(a\sqrt{K_0^2\epsilon_R-h_P^2})J_0'(b\sqrt{K_0^2\epsilon_R-h_P^2})\\ & -bJ_0(a\sqrt{K_0^2\epsilon_R-h_P^2})N_0'(b\sqrt{K_0^2\epsilon_R-h_P^2})-aN_0(b\sqrt{K_0^2\epsilon_R-h_P^2})J_0'(a\sqrt{K_0^2\epsilon_R-h_P^2})]\end{aligned} \tag{27}$$

$$\begin{aligned}\beta'(h_P) = {} & -h_P(K_0^2\epsilon_R-h_P^2)^{-1/2}[bJ_0(a\sqrt{K_0^2\epsilon_R-h_P^2})N_0''(b\sqrt{K_0^2\epsilon_R-h_P^2})+aJ_0'(a\sqrt{K_0^2\epsilon_R-h_P^2})N_0'(b\sqrt{K_0^2\epsilon_R-h_P^2})\\ & -bN_0(a\sqrt{K_0^2\epsilon_R-h_P^2})J_0''(b\sqrt{K_0^2\epsilon_R-h_P^2})-aJ_0'(b\sqrt{K_0^2\epsilon_R-h_P^2})N_0'(a\sqrt{K_0^2\epsilon_R-h_P^2})].\end{aligned} \tag{28}$$

The far-field strength is a function of the variables R, B, P, γ, and θ. Thus

$$| H_\phi(R, \theta) | = 2c\epsilon_0 \left| 1 - \frac{1}{\gamma^2} \right| V_0/\pi^2 RB \, | L | \tag{29}$$

$$L = H_1^{(1)}(B \cos\theta)\left[1 - \frac{1}{\gamma^2} - \sin^2\theta\right]\left[J_0\left(b\sqrt{1 - \frac{1}{\gamma^2} - \sin^2\theta}\right) N_0\left(BP\sqrt{1 - \frac{1}{\gamma^2} - \sin^2\theta}\right) - J_0\left(BP\sqrt{1 - \frac{1}{\gamma^2} - \sin^2\theta}\right) N_0\left(B\sqrt{1 - \frac{1}{\gamma^2} - \sin^2\theta}\right)\right]$$
$$+ \left(1 - \frac{1}{\gamma^2}\right) \cos\theta H_0^{(1)}(B \cos\theta) \sqrt{1 - \frac{1}{\gamma^2} - \sin^2\theta}\left[J_0\left(BP\sqrt{1 - \frac{1}{\gamma^2} - \sin^2\theta}\right) N_1\left(B\sqrt{1 - \frac{1}{\gamma^2} - \sin^2\theta}\right) - N_0\left(BP\sqrt{1 - \frac{1}{\gamma^2} - \sin^2\theta}\right) J_1\left(B\sqrt{1 - \frac{1}{\gamma^2} - \sin^2\theta}\right)\right]. \tag{30}$$

c is the velocity of light in a vacuum. The quantity plotted is

$$h_\phi(\theta) = \frac{|H_\phi(R, \theta)|}{2c\epsilon_0 V_0/\pi^2 R}.$$

Plots are made for various values of γ for fixed B and P. Examples involving positive as well as negative ϵ_R are presented. The field strength for negative ϵ_R is flatter as a function of θ and doesn't show the sharp peaking apparent in the positive ϵ_R cases. Increasing the ratio a/b while keeping $K_0 b$ constant tends to shift the peaks to higher values of θ.

This is understandable since increasing the ratio a/b corresponds to making the plasma sheath thinner. As $a/b \to 1$ the plasma thickness approaches zero. Decreasing the thickness of the sheath corresponds to an approach to free space conditions outside the antenna which in the limit of zero sheath thickness becomes a perfect traveling-wave antenna.

For long but finite cylindrical antennas whose main lobe is at large values of θ the same effect in the far-field pattern should be noticed. Thus a practical effect of the plasma sheath surrounding a vehicle designed to radiate like a long cylindrical antenna would be to shift the main lobe away from end-fire in the direction of broadside.

A simplified, semiphysical way of looking at this situation is to think of rays emenating from the gap as being bent toward the normal when reaching the plasma-air interface, thus shifting the pattern toward broadside. For plasmas with negative permittivity the result would be even more dramatic due to the loss in the medium which would affect rays at larger angles more because of increased path length in the plasma. The result should be a further shift toward normal plus smaller magnitudes at the peaks. These effects seem to be borne out by the curves presented (Figs. 4–14).

In conclusion, far-field solutions, as well as surface wave solutions, have been obtained for a cylindrical antenna surrounded by a plasma sheath and fed across an infinitesimal gap. The surface waves decay away from the plasma-air interface, the rate of decay increasing as ω/ω_P increases. The far-field patterns show sharper peaking when the permittivity is positive and an increase in ratio of cylindrical radius to the radius of cylinder-plus-plasma tends to shift the peaks toward higher angles.

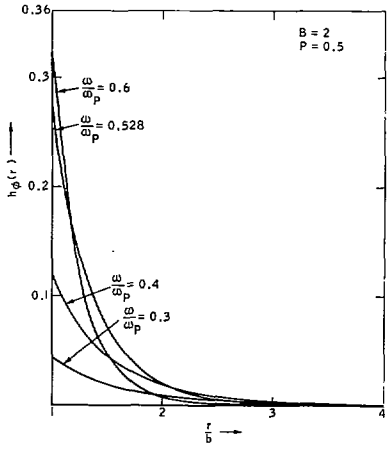

Fig. 4. Surface wave fields.

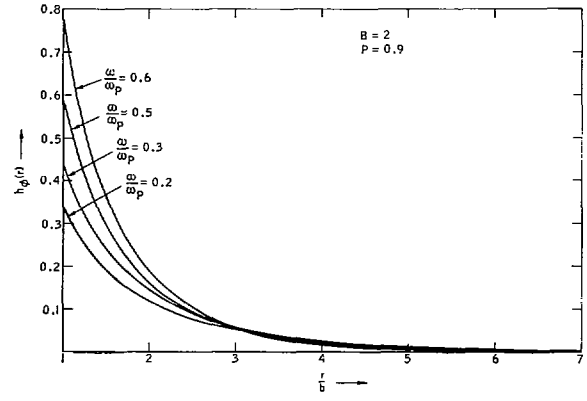

Fig. 5. Surface wave fields.

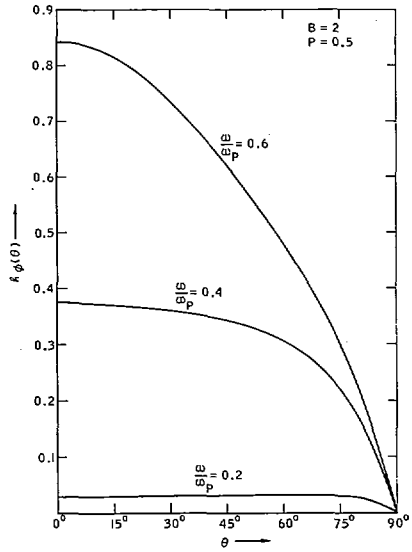

Fig. 6. Far-field patterns.

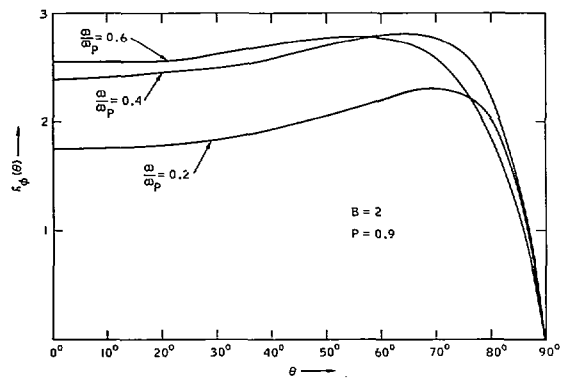

Fig. 7. Far-field patterns.

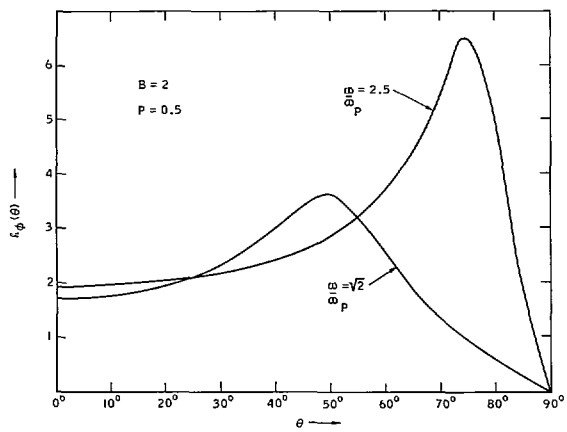

Fig. 8. Far-field patterns.

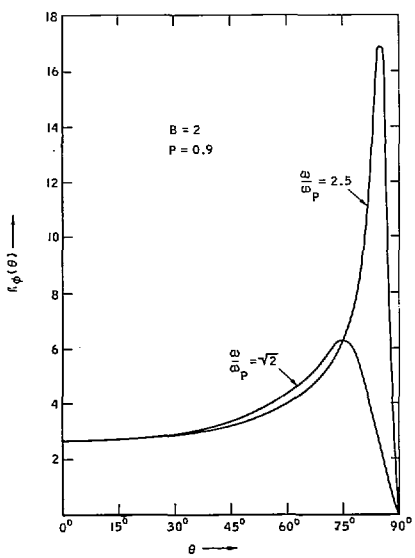

Fig. 9. Far-field patterns.

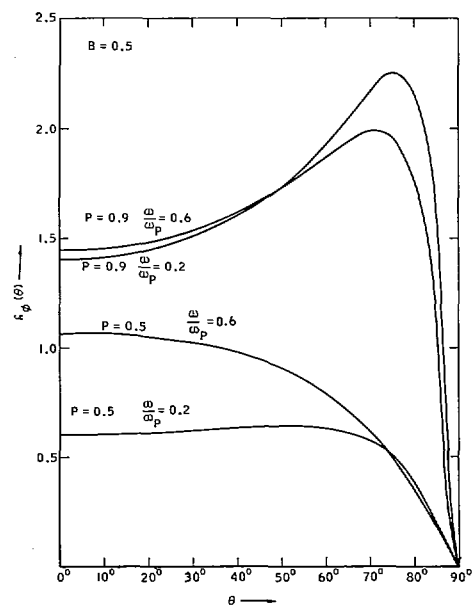

Fig. 10. Far-field patterns.

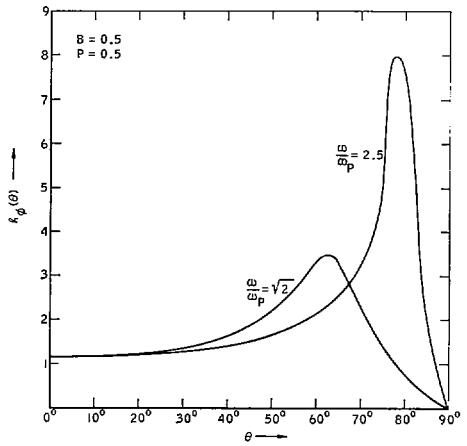

Fig. 11. Far-field patterns.

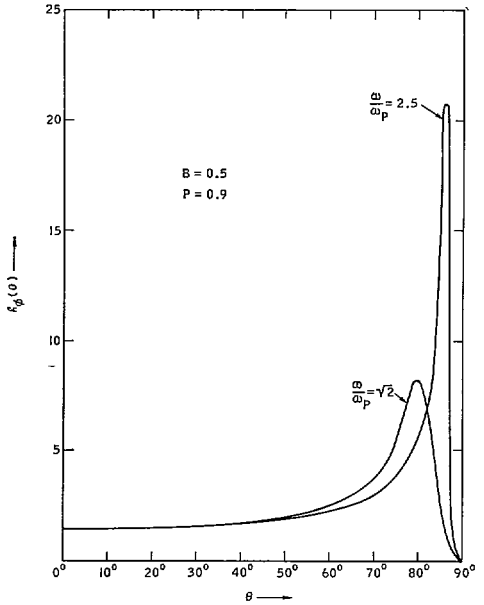

Fig. 12. Far-field patterns.

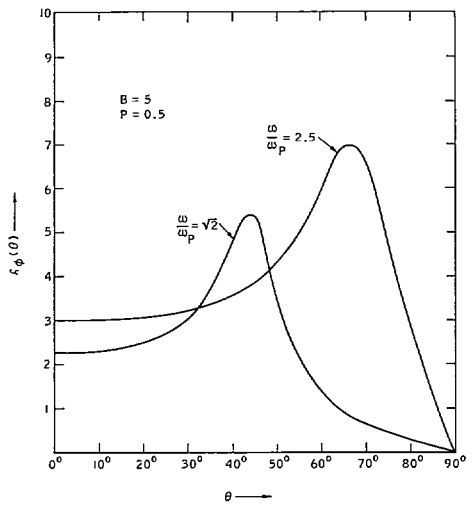

Fig. 13. Far-field patterns.

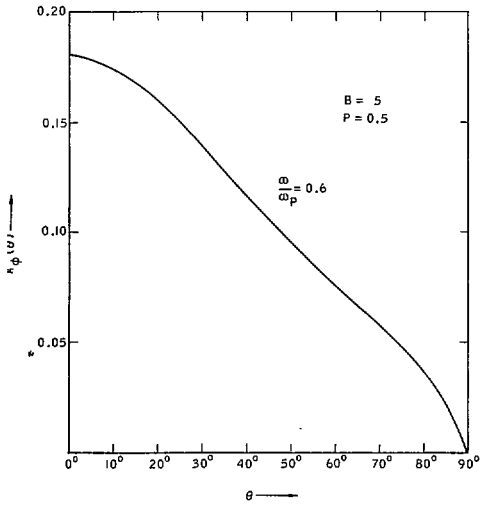

Fig. 14. Far-field patterns.